

# A Detailed Experimental and DFT Study on Silver-6-Aminobenzimidazole Surface Complex- An Endeavour in prognosis of Anti-Cancerous Materials

ShaikJaheerBasha<sup>1</sup>, S.P.VijayaChamundeeswari<sup>2</sup>, H.Umamahesvari<sup>3</sup>

<sup>1</sup>Centre for Crystal Growth. VIT University, Vellore, Tamilnadu, India.

<sup>2</sup>Centre for Crystal Growth. VIT University, Vellore, Tamilnadu, India.

<sup>3</sup>Department of Physics, Sreenivasa Institute of Technology and Management Studies(Autonomous), Chittoor, Andrapradesh, India.

## Abstract

The advancement on the low dimensional nanomaterials brings the quick development of nanocommunity. The nanotechnology has opened up new wildernesses in materials science and designing to address this difficulty by making new materials, especially drugnanometal-surface complexes. The versatile tool to study the characteristics of such materials is Quantum chemical method, Density Functional theory (DFT) is a standout amongst the most mainstream way to deal with quantum mechanical many body electronic structure computations of molecular and condensed matter systems. So in the present Investigation, a detailed experimental and theoretical study on the Silver 6-aminobenzimidazole surface complex is done. Silver nanoparticles (AgNP) have wider applications in many fields and particularly in medicine for drug delivery, medical imaging and diagnosis. Benzimidazole class of compounds are found to have anti-cancer effect. Hence it is imperative to study the interaction of silver with 6-aminobenzimidazole. In the present study, Silver nanoparticles are prepared by chemical reduction method using trisodium citrate as reducing agent. The silver-6-aminobenzimidazole surface complex are prepared in the ratio 1:1. The synthesized surface complex has been characterized by UV-Vis spectroscopy, FTIR spectroscopy, Surface Enhanced Raman Spectroscopy (SERS), Scanning electron microscopy (SEM) and Energy-dispersive X-ray spectroscopy (EDAX). The silver-6-aminobenzimidazole surface complex structure is optimized by Density Functional Theoretical (DFT) calculations using B3LYP method with 6-311G as basis set. Calculated normal modes of frequencies of the compound from DFT calculations are compared with data obtained from SERS and FT-IR spectrum.

**Key words:** DFT, Silver nano particle, Surface Complex, SERS and, SEM, Silver-6-Aminobenzimidazole

## 1. INTRODUCTION

There are many number of registered drugs which are derivatives of benzimidazole class of compounds. The heterocyclic aromatic organic compound, 6-aminobenzimidazole is a promising class of biologically active chemical compound. This important group of substances has found practical applications in a number of fields, particularly in medicine as analgesic, anti-inflammatory, antibacterial, antifungal, antiviral, anticancer, antiulcer and antihypertensive[1,2,3,4,5]. Many synthesized the compounds of benzimidazole [6,7,8,9,10,11]. Few Quantum chemical calculations were also performed [12,13,14,15,16,17]. Apart many studies are reported the medicinal properties such as in wound healing, drug delivery, cancer therapy, diagnostics and therapeutics of Silver nanoparticles[18,19,20,21] Now-a-days many commercial products such as ointments, soaps, cosmetics, etc., are found to have silver nanoparticles. Silver nanoparticles are also used for medical imaging and targeted drug delivery. Hence, it is interesting and important to study the interaction of 6-aminobenzimidazole with silver nanoparticles. A detailed experimental and theoretical study on silver 6-aminobenzimidazole surface complex is carried out in this paper.

## 2. EXPERIMENTAL DETAILS

### 2.1 Materials and Methods

The 6-aminobenzimidazole was purchased from Sigma-Aldrich chemical company (USA) with the stated purity of

95% and it was used without any further purification. Analytical grade Silver nitrate ( $\text{AgNO}_3$ ) and Trisodium citrate are used. Deionized water is used throughout the synthesis process.

### 2.1.1 Chemical Reduction Method

Chemical reduction method is the most frequently applied method for the synthesis of metal nanoparticles of several nanometers[22,23]. Commonly used reducing agents are borohydride, citrate, and elemental hydrogen. Initially, the reduction of various complexes with metal ions leads to the formation of copper atoms. It is followed by agglomeration into oligomeric clusters. These clusters eventually lead to the formation of colloidal silver nanoparticles. The nanoparticles synthesized by this method have wide particle size distribution. Here, trisodium citrate is used as reducing agent. It not only acts as reducing agent but also as stabilizer which controls the grain growth and makes the metal nanoparticles to be in nano regime itself [24].

### 2.1.2 Synthesis of AgNPs - 6-aminobenzimidazole Surface Complex

Silver nanoparticles are synthesised by chemical reduction method as follows. 10 ml of aqueous solution 0.001M of Silver nitrate ( $\text{AgNO}_3$ ) is kept on stirrer approximately at 60°C. 2 ml 1% aqueous solution of trisodium citrate is added drop by drop with continuous stirring. The solution is kept undisturbed for a week and the colourless solution turned to yellow colour which indicates the conversion of metal ions into nanoparticles. Initially, the metal ions are reduced to atoms. Then agglomeration of these atoms

results in formation of cluster. This results in formation of silver nanoparticles. This process is slow process, but nanoparticles synthesised by this method is highly stable and there is no tedious procedures involved in this method. To the above prepared silver nanoparticles solution 0.001M of aqueous solution of 6-aminobenzimidazole is added with continuous stirring for 4 minutes. Then the prepared sample is subjected to microwave irradiation for 30 seconds. Thus the AgNps-6-aminobenzimidazole surface complex is prepared

## 2.2. CHARACTERIZATION TEQNIQUES:

### 2.2.1 FT-IR Spectrometer

FT-IR spectrum of the sample was recorded with the JASCO UV Visible Spectrophotometer (V-670 PC). In this technique the sample is simultaneously exposed to complete range of IR frequencies i.e., from  $500\text{ cm}^{-1}$  to  $4000\text{ cm}^{-1}$ . Those frequencies which are not absorbed by the sample is taken as sample beam that attains 100% transmittance recorded in the detector.

### 2.2.2 Surface Enhanced Raman Spectroscopy (SERS)

FT-Raman spectrometer which provides an excitation wavelength of 1064 nm is used. Molecules adsorbed on the surface of the nanomaterial give rise to a phenomenon called surface enhanced Ramanscattering (SERS) in which the Raman signals are found to be highly enhanced with an intensity being  $10^6$  times that of the normal Raman ones. This effect has gained attention from both basic and practical viewpoints. It takes Raman spectroscopy to the rank of single molecule detection technique. The resulting SERS spectra contain the structural information of vibrational spectroscopy with the ability of detecting molecules up to their attomolar level. The production of SERS active substrates that are stable and have controlled roughness and reproducible structure has been a challenging problem to the SERS spectroscopists. A variety of methods employing different types of liquid and solid SERS substrates have been applied for the detection of enhanced Raman signals. In most of these substrates, silver is often the metal of choice, although other metals can also be used (e.g., copper and gold). Fabrication of SERS active thin film substrates based on the sol-gel processing technology has been reported in the literature by various researchers. In this technique, a sol and then a gel are produced through the subsequent hydrolysis and condensation of the alkoxy silane precursor. Further drying of the gel forms a porous silica structure which is known as a xero gel. This kind of substrates combine the high activity of colloids with the chemical and mechanical stability of sol-gel film and find their application in many areas, particularly marine water analysis. The main advantages of these xero gel films are first, good mechanical, chemical and optical properties and second that porosity pore size and surface polarity are controllable by choice of the starting material of the sol and processing parameters.

### 2.2.3 UV- Vis Spectroscopy

The UV-Vis spectrum of the sample is measured by JASCO UV Visible Spectrophotometer (V-670 PC). It is also referred as absorption spectroscopy. The

wavelengths of absorption peaks have a strong relation with the types of bonds in a given molecule and are valuable in determining the functional groups within a molecule. The absorption in the visible region of light directly related to the colour in which the substance is identified.

### 2.2.4 Scanning Electron Microscopy (SEM)

The SEM image of the sample provides the information about its surface morphology, particle size and structures.

## 3. COMPUTATIONAL DETAILS

The DFT calculations of AG@6-aminobenzimidazole are performed with B3LYP method using 6-311G basis set. The structure and vibrational frequencies of the molecule are determined with DFT.

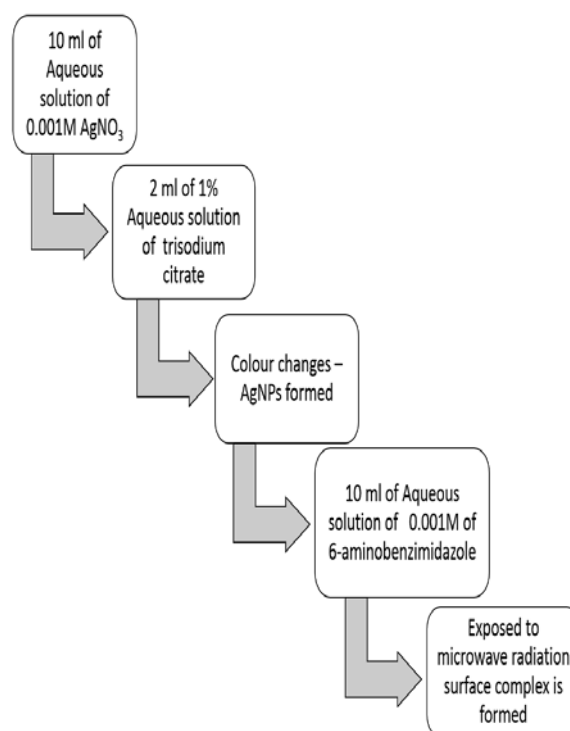


Fig.1.1. Synthetic Scheme of silver 6-aminobenzimidazole surface complex

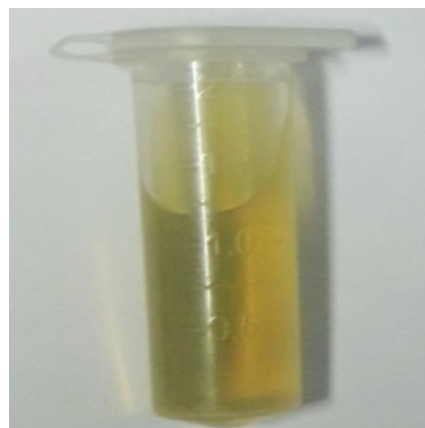


Fig. 1.2. Silver nanoparticles

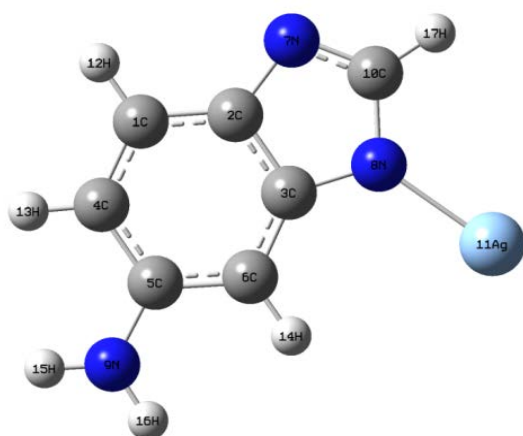
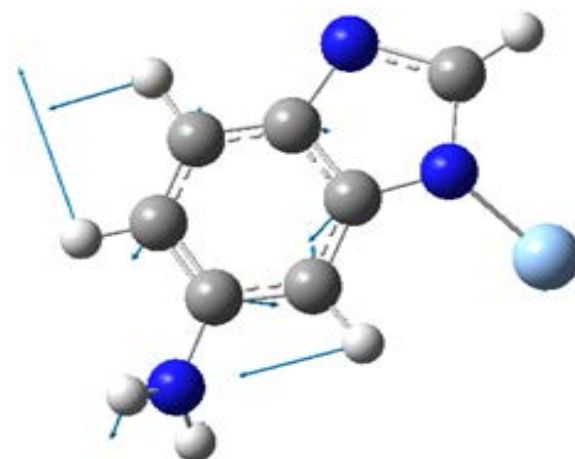


Fig .1.3. Optimized structure with numbering scheme of Ag@6-aminobenzimidazole



c) Frequency 1702.30  $\text{cm}^{-1}$

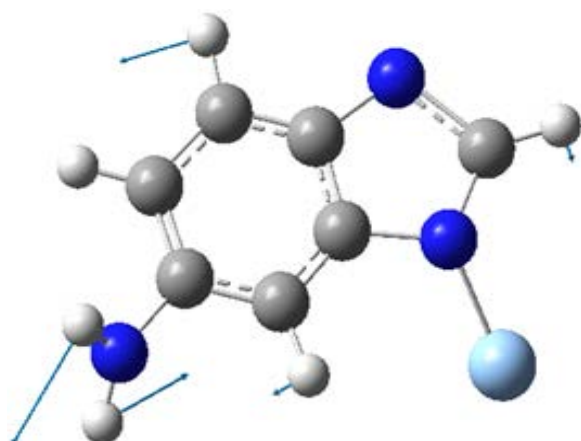
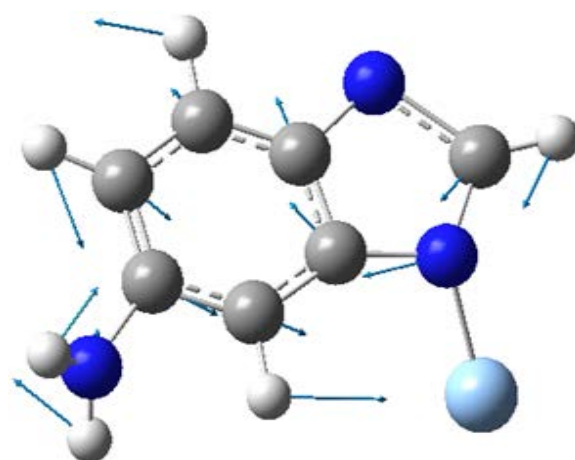
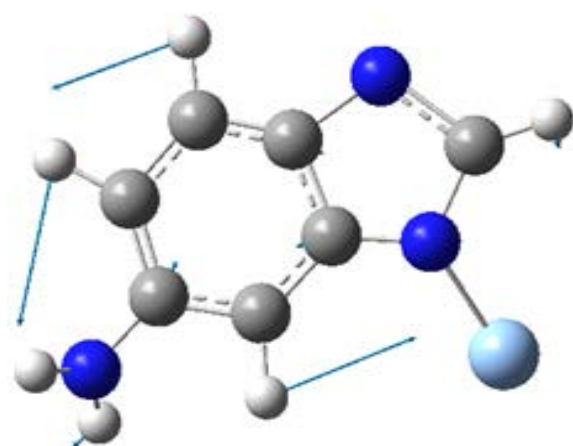


Fig.1.4. Vibrational Frequency assignments of Ag@6-aminobenzimidazole

a) Frequency (1338.46  $\text{cm}^{-1}$ )



d) Frequency 580.23  $\text{cm}^{-1}$



a) Frequency 1557.30  $\text{cm}^{-1}$

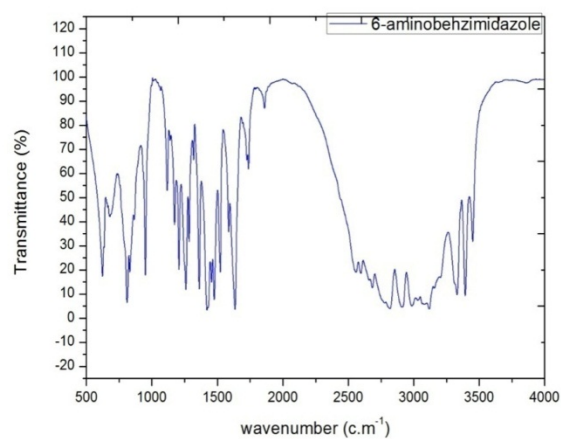
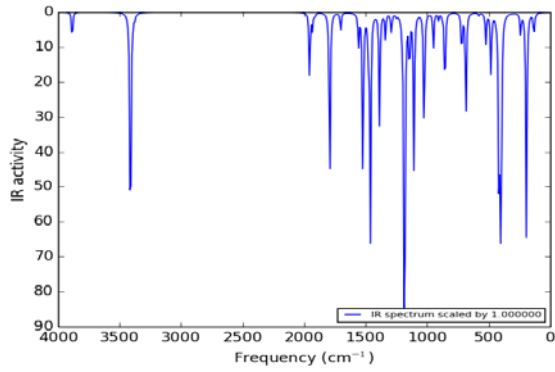
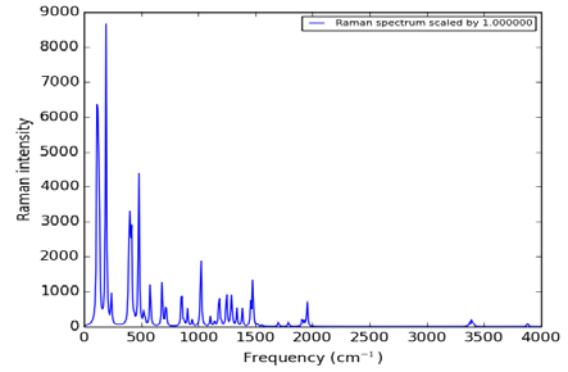


Fig 1.5 Experimental FT-IR spectrum of 6-aminobenzimidazole



**Fig. 1.6** Theoretical FT-IR spectrum of Ag@6-aminobenzimidazole



**Fig.2,2.** Theoretical FT-Raman spectrum of Ag@aminobenzimidazole

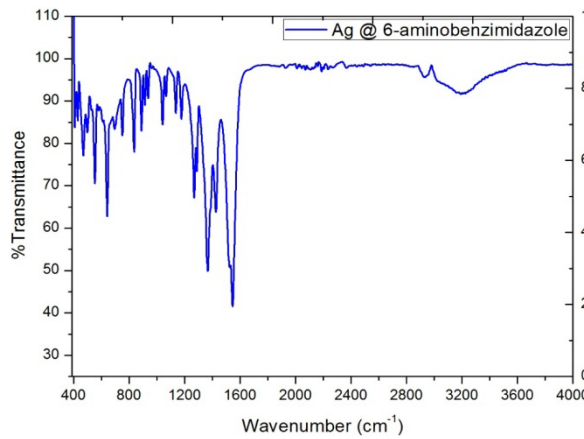


**Fig 1.7** Experimental FT-IR spectrum of silver-6-aminobenzimidazole surface complex

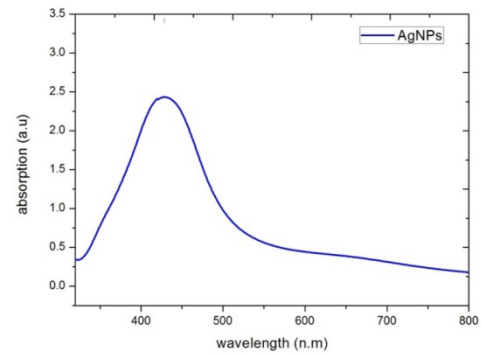


**Fig 2.3** absorption spectrum of silver nanoparticles

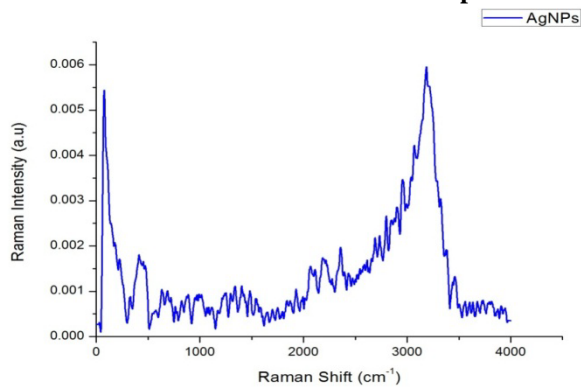


**Fig 1.8.** FT-Raman spectrum of AgNPs

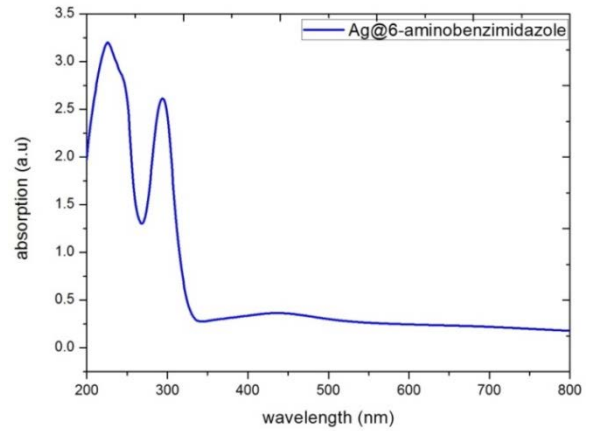


**Fig 2.4.** Absorption spectrum of Silver-6-aminobenzimidazole surface complex

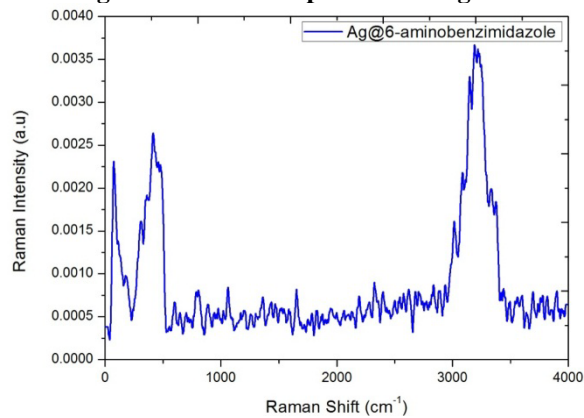


**Fig 2.1** Experimental FT-Raman Spectrum of Ag@6-aminobenzimidazole

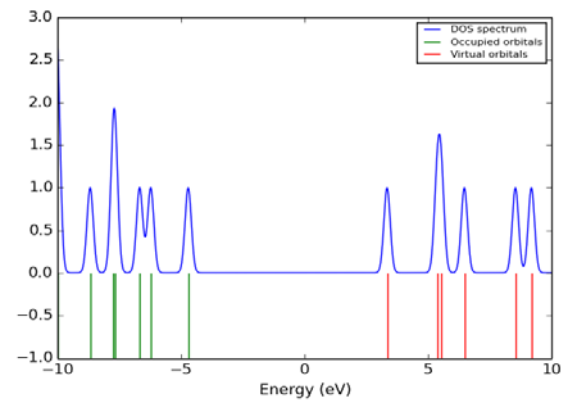


**Fig 2.5.** Electronic Density of states (DOS) plots of DFT optimised AG@6aminobenzimidazole

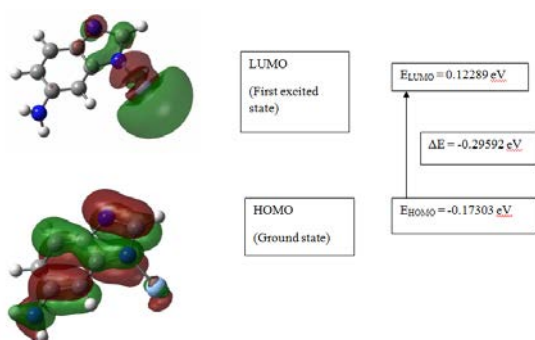


Fig 2.6 HOMO &amp; LUMO Structures

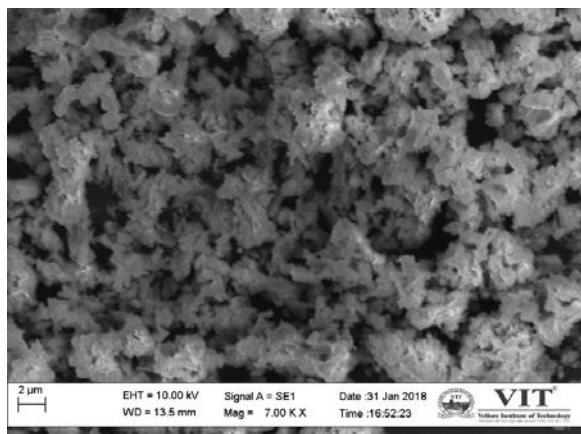
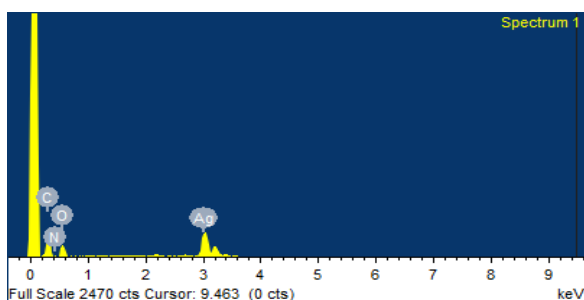


Fig 2.7. SEM image of silver-6-ABI surface complex



Element	Weight%	Atomic%
C K	12.12	29.5
N K	11.14	23.24
O K	17.01	31.08
Ag L	59.73	16.18
Totals	100	

Fig.2.8 EDAX of silver-6-ABI

#### 4. RESULTS AND DISCUSSIONS

##### 4.1 Vibrational Frequencies and Assignment of Ag@6-aminobenzimidazole

The molecular arrangement of the atoms in AgNps@6-Aminobenzimidazole is illustrated in Fig.1.3. The geometrical parameters like bond length, bond angle and dihedral angle of silver 6aminobenzimidazole compound are carried out by B3LYP/6-311G (d, p) method.

The observed experimental FT-IR and FT-Raman frequencies of silver-6-aminobenzimidazole were

compared with the calculated theoretical frequencies. The compound had 44 vibrational frequencies. For the calculated theoretical frequency at  $480.15\text{ cm}^{-1}$  there is an experimental FT-IR frequency at  $476.68\text{ cm}^{-1}$  which corresponds to the combination of vibrations of CCC in plane bending, CCN in-plane bending, N-C-NH<sub>2</sub> in-plane bending, and CN stretching. For the calculated theoretical frequency at  $533.98\text{ cm}^{-1}$  there is an experimental FT-IR frequency observed at  $555.54\text{ cm}^{-1}$  that corresponds to the vibrations of CCC out of plane bending and CNC out of plane bending. For the calculated frequency at  $580.23\text{ cm}^{-1}$  there exists an experimental FT-Raman frequency at  $612.26\text{ cm}^{-1}$  which is resulted from the vibrations of CCC out of plane bending, NCC out of plane bending and CC stretching.

For the theoretical frequency at  $876.74\text{ cm}^{-1}$  there comes an experimental FT-IR and FT-Raman frequencies at  $885.08\text{ cm}^{-1}$  and  $892.60\text{ cm}^{-1}$  respectively, they are resulted from the vibrations of CCC in-plane bending and CN stretching. For the observed frequency at  $1023.96\text{ cm}^{-1}$ , there is an experimental FT-IR and FT-Raman frequencies seen at  $1044.37\text{ cm}^{-1}$  and  $1060.99\text{ cm}^{-1}$  and they are exhibited by the vibrations of CC stretching. For  $1142.98\text{ cm}^{-1}$ , there is an experimental FT-IR frequency at  $1138.80\text{ cm}^{-1}$  which is resulted from the vibrations of CH in-plane bending and CC stretching. For  $1289.34\text{ cm}^{-1}$ , there found an experimental FT-IR frequency at  $1269.27\text{ cm}^{-1}$  which is caused by the vibrations of CC stretching and CN stretching. For  $1386.32\text{ cm}^{-1}$ , there is an experimental FT-IR and FT-Raman frequency at  $1362.97\text{ cm}^{-1}$  and  $1368.59\text{ cm}^{-1}$  respectively, they related to the vibrations of CC stretching and CH in-plane bending. Finally, for  $1460.12\text{ cm}^{-1}$  there exists an experimental FT-IR frequency at  $1428.57\text{ cm}^{-1}$  that attributes to the vibrations of CNN asymmetric stretching and NH<sub>2</sub> rocking. Thus the theoretical calculations are found to be in well agreement with the experimental results. The theoretical and the experimental. A slight change in the peak intensity or the position of the peak might happen when comparing calculated to experimental values which might be attributed to solvent effect.

##### 4.2. UV-VIS SPECTRAL ANALYSIS

The absorption spectrum of Silver nanoparticles is shown in the Fig.2.3. In the graph, there is an absorption peak at  $430\text{ nm}$  which shows the formation of silver nanoparticles. The absorption is surface Plasmon resonance at visible region and it can be seen that the sample appears in yellowish green colour from Fig. 1.2. Fig.2.4 shows the absorption spectrum of silver-6-aminobenzimidazole surface complex. The two absorption peak at  $230\text{ nm}$  and  $300\text{ nm}$  which correspond to 6-aminobenzimidazole (6-ABI) and a relatively weak peak at  $430\text{ nm}$  shows the silver nanoparticles interaction with 6-ABI

##### 4.3. Energy Gap

The energy gap of conductors that is metals is zero eV in bulk silver and it is reported that  $2.6\text{ eV}$  for silver dimer nanoparticles [25]. In the present investigation it is about  $0.29592\text{ eV}$ . The increase in the band gap of the Ag nanoparticles with the decrease in particle size may be due to a quantum confinement effect [26].

#### 4.4. SEM and EDAX Analysis

To study the morphological aspects such as shape, size of the particles etc., of the sample SEM is carried out and EDAX was recorded for chemical composition information of the sample.

The SEM image of Silver-6-ABI is shown in Fig 2.7. It seems to be strongly agglomerated. The reason for the large grain size distribution might be related to grain growth condition and densification of the crystallites. EDAX analysis shows that Ag is present in weight ratio of 59% as given in the Fig.2.8.

Table.1.Optimized Frequencies of Silver-6-Aminobenzimidazole

Mode no.	Theoretical Wavenumbers (cm <sup>-1</sup> )			Experimental Wavenumbers (cm <sup>-1</sup> )		Assignment mode
	B3LYP/6-311G			FT-IR	FT-Raman	
	Scaled	I <sub>IR</sub>	I <sub>R</sub>			
1	116.92	0.6240	2.4601			
2	132.52	7.2017	1.6953			Butterfly
3	192.48	66.1085	6.4381			
4	239.81	6.4653	1.0502			γ CCN + γ CCC
5	390.81	5.6567	2.9862			γ NH
6	399.07	72.4012	11.2126			
7	414.62	64.7157	13.0399		416.61	
8	438.93	0.7318	0.7660			γ CCC
9	480.15	18.9767	23.9008	476.68		β CCC + β CCN + β N-C-NH <sub>2</sub> + ν CN
10	521.85	8.7608	1.9215			r NH <sub>2</sub> + β CCN + γ CCC
11	533.98	0.4250	1.5460	555.54		γ CCC + γ CNC
12	580.23	0.9463	10.3102		612.26	γ CCC + γ NCC + ν CC
13	684.26	32.7290	15.6244	633.63		ω NH <sub>2</sub>
14	714.45	5.6489	4.5960			γ CCC + γ NCN
15	721.45	6.9197	4.2724	757.79		γ CCC + ω NH <sub>2</sub>
16	854.57	26.1965	23.9843	835.88		ν CC + ν CN + β NCN
17	876.94	1.1943	2.6485	885.08	892.60	β CCC + ν CN
18	906.82	2.0521	9.8942			γ CH
19	948.29	10.9659	4.5896			γ CH
20	1023.96	39.6160	65.4951	1044.37	1060.99	ν CC
21	1106.49	44.7168	8.8306			r NH <sub>2</sub> + ν CN
22	1142.98	16.9306	5.9139	1138.08		β CH + ν CC
23	1183.54	126.9337	43.7193	1175.56		
24	1202.88	2.6213	3.8356			ν CN + β NH + β CCC
25	1248.09	1.0414	51.9231			β CH + β NH + ν CC + ν CN
26	1289.34	5.9108	42.9313	1269.27		ν CC + ν CN
27	1299.73	0.5476	11.6482			ν CC
28	1338.46	7.5104	26.3021			
29	1386.32	33.6443	29.1697	1362.97	1368.59	ν CC + β CH
30	1460.12	65.6366	40.2525	1428.57		ν <sub>asym</sub> CNN + r NH <sub>2</sub>
31	1477.73	11.6051	95.9027			ν CC + β CH + ν <sub>asym</sub> CNN
32	1521.28	53.9276	4.8682			ν CN + ρ NH <sub>2</sub>
33	1557.30	9.8847	3.5538	1541.01		ν CC
34	1702.30	5.8349	13.3765		1662.56	
35	1790.53	54.9710	15.7708			
36	1911.74	1.2503	35.8352			
37	1932.08	4.7608	17.3171			
38	1954.55	20.3434	105.3850			
39	3355.58	0.2111	15.3705	3227.71	3231.67	
40	3374.57	1.1835	66.1115			
41	3393.51	1.5714	161.5697			
42	3411.04	82.3818	75.1831			ν <sub>sym</sub> NH <sub>2</sub>
43	3884.11	9.0089	140.1084		3904.28	
44	4104.58	5.8863	60.3461			

I<sub>IR</sub>- IR intensity (km mol<sup>-1</sup>); I<sub>Ra</sub>- Raman intensity (a.u); ν-stretching; β- in plane bending; γ- out of plane bending; ρ - scissoring; ω- wagging; r- rocking

### CONCLUSION

The silver-6-aminobenzimidazole surface complex has been synthesized by chemical reduction method and the theory behind FT-IR spectroscopy and FT-Raman spectroscopy are discussed in detail. The experimental techniques used are explained briefly. The molecular structural parameters of the optimized geometry of silver-6-aminobenzimidazole have been obtained from DFT/B3LYP level of calculation and the computed geometries are benchmarks for predicting structural data. The SEM image and EDAX report are analysed which shows 59% of silver by weight percentage and the structure of Ag@6-aminobenzimidazole optimized and the Frequency calculated by DFT is compared with the Experimental data from FT-IR and FT-Raman Spectra of the compound. And also, some of the normal mode figures of the corresponding frequencies are illustrated. The frequencies calculated theoretically by DFT method are found to be in good agreement with the experimental results.

### REFERENCES

- [1] Yerragunta, V., Patil, P., Srujana, S., Devi, R., Gayathri, R., Srujana, D., A Review, *Pharma Tutor*, 2014., 2, 109-113
- [2] Velík, J., Baliharová, V., Fink-Gremmels, J., Bull, S., Lamka, J., Skálová, L., *Research in Veterinary Science*, 2004, 76, 95-108.
- [3] Merino, G., Jonker, J.W., Wagenaar, E., Pulido, M.M., Molina, A.J., Alvarez, A.I., Schinkel, A.H., *Drug Metabolism and Disposition*, 2005, 33, 614-618.
- [4] Lam, L.T., Zhang, H., Xue, J., Levenson, J.D., Bhathena, A., *Cancer Cell International*, 2015, 15, 1-9.
- [5] Shaker, Y.M., Omar, M.A., Mahmoud, K., Elhallouty, S.M., El-Senousy, W.M., Ali, M.M., Mahmoud, A.E., Abdel-Halim, A.H., Soliman, S.M., El Diwani, H.I., *J. of Enzyme Inhibition and Medicinal Chemistry*, 2015, 30, 826-845
- [6] Ansari, K.F., Lal, C., *European Journal of Medicinal Chemistry*, 2009, 44, 4028-4033
- [7] Sachin Kale, Kale MK, Biyani KR, *Synthesis Of Some New Benzimidazole Acetic Acid Derivatives And Evaluation For Their Antimicrobial And Antitubercular Activities*, *International Journal Of Biomedical And Advance Research*, 2013, 4(5), 321-327.
- [8] Lacey, E., *International Journal for Parasitology*, 1988, 18, 885-936.
- [9] Velík, J., Baliharová, V., Fink-Gremmels, J., Bull, S., Lamka, J., Skálová, L., *Research in Veterinary*, 2004 76, 95-108.
- [10] Nguyen, K.M., Largeron, M., *Chemistry*, 2015, 21, 12606-12610
- [11] Alp, M., Gurkan-Alp, A.S., Ozkan, T., Sunguroglu, A., *Zeitschrift für Naturforschung, C., Journal of Biosciences*, 2015, 70, 79-85.
- [12] Wang, X.B., Wu, R.M., Liu, M.H., Zhang, L.L., Lin, L., *GuangPuXue Yu GuangPu Fen Xi = Guang Pu*, 2015, 35, 1562-1566.
- [13] Diaz, C., Llovera, L., Echevarria L., Hernández FE, *Assessment of the tautomeric population of benzimidazole derivatives in solution: a simple and versatile theoretical-experimental approach*, *Journal of Computer-aided Molecular Design*, 2015, 29(2), 143-154.
- [14] Obayes, H.R., Alwan, G.H., Alobaidy, A.H., Al-Amiery, A.A., Kadhum, A.A., Mohamad, A.B., *Chemistry Central Journal*, 2014, 8, 1-8.
- [15] Thiarié, D.D., Khonté, A., Diop, A., Cissé, L., Coly, A., Tine, A., Delattre F., *J. of Mole. Liquids*, 2015, 211, 640-646.
- [16] Sas, E.B., Kurt, M., Karabacak, M., Poyimozhi, A., Sundaraganesan, N., *J. of Mole. Structure*, 2015, 1081, 506-518.
- [17] Sudha, S., Karabacak, M., Kurt, M., Cinar, M., Sundaraganesan, N., *Spectrochimica Acta Part A: Molecular and Biomolecular Spectroscopy*, 2011, 84, 184-195.
- [18] Rajkiran Reddy Banala., Veera Babu Nagati., Pratap Reddy Karnati., *Saudi Journal of Biological Sciences*, 2015, 22, 637-644
- [19] Mohamed, S., Abdel-Aziz., Mohamed, S., Shaheen., Aziza, A., El-Nekeety, Mosaad, A., Abdel-Wahhab., *Journal of Saudi Chemical Society*, 2014, 18, 356-363.
- [20] Chandrasekaran Rajkuberan., Seetharaman Prabukumar., Gnanasekar Sathishkumar., Arockiasamy Wilson., Keepanan Ravindran., Sivaperumal Sivaramakrishnan., *Journal of Saudi Chemical Society*, 2017, 21, 911-919.
- [21] Agbaje Lateefa et al., *Journal of Taibah University for Science*, 2016, 10(4), 551-562
- [22] Veshara Malapermal., Izel Botha., Suresh Babu Naidu Krishna., Joyce Nonhlanhla Mbatha., *Saudi Journal of Biological Sciences*, 2017, 24, 1294-1305.
- [23] Suriati Ghazali., Mariatti Jaafar., Azizan A., *International Journal of Automotive and Mechanical Engineering*, 2014, 10(1), 1920-1927.
- [24] Krutagn Patel., Bhavesh Bharatiya., Tulsi Mukherjee., Tejal Soni., Atindra Shukla., Suhagia, B.N., *Journal of Dispersion Science and Technology*, 2017, 38, 626-631.
- [25] Yukna, J., *United Microform*, 2007, 55-56.
- [26] Yang, J.P., Meldrum, F.C., Fendler, J.H., *J. Physical Chemistry*, 1995, 99, 5500-5504.